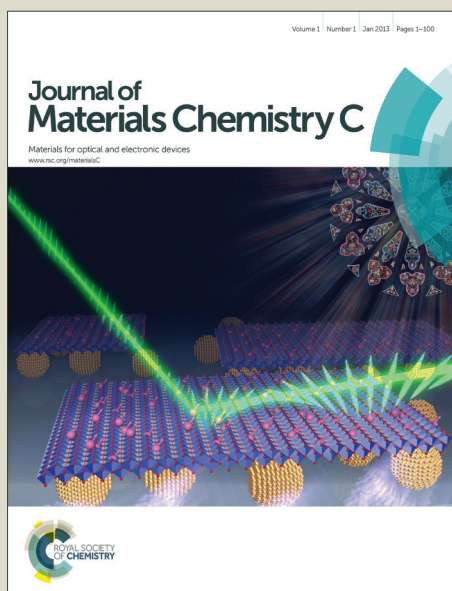


Journal of Materials Chemistry C

Accepted Manuscript



This is an *Accepted Manuscript*, which has been through the Royal Society of Chemistry peer review process and has been accepted for publication.

Accepted Manuscripts are published online shortly after acceptance, before technical editing, formatting and proof reading. Using this free service, authors can make their results available to the community, in citable form, before we publish the edited article. We will replace this *Accepted Manuscript* with the edited and formatted *Advance Article* as soon as it is available.

You can find more information about *Accepted Manuscripts* in the [Information for Authors](#).

Please note that technical editing may introduce minor changes to the text and/or graphics, which may alter content. The journal's standard [Terms & Conditions](#) and the [Ethical guidelines](#) still apply. In no event shall the Royal Society of Chemistry be held responsible for any errors or omissions in this *Accepted Manuscript* or any consequences arising from the use of any information it contains.

Manipulation of Multiple-responsive Fluorescent Supramolecular Materials Based on Inclusion Complexation of Cyclodextrins With Tyloxapol

Jinglin Shen ^a, Jinyu Pang ^b, Tomasz Kalwarczyk ^c, Robert Hołyst ^c, Xia Xin ^{a, d, *}, Guiying Xu ^{a, d},

Xiaoyu Luan ^a, Yingjie Yang ^a

^a *Key Laboratory of Colloid and Interface Chemistry (Shandong University), Ministry of Education,*

Shanda nanlu No. 27, Jinan, 250100, P. R. China

^b *Shanxi Transportation Research Institute, Taiyuan 030006*

^c *Department III, Institute of Physical Chemistry, Polish Academy of Sciences, Kasprzaka 44/52,*

01-224 Warsaw, Poland

^d *National Engineering Technology Research Center for Colloidal Materials, Shandong University,*

Shanda nanlu No. 27, Jinan, 250100, P. R. China

Abstract

Fluorescent supramolecular hydrogel was prepared by α -cyclodextrin (α -CD) and Tyloxapol, which can be considered as an oligomer of the nonionic surfactant polyoxyethylene tert-octylphenyl ether (Triton X-100, TX-100) with a polymerization degree below 7. For comparison, both Tyloxapol and TX-100 were selected to form hydrogels with α -CD to get more information about the interaction between different types of surfactants and cyclodextrin. These hydrogels have been

* Author to whom correspondence should be addressed, E-mail: xinx@sdu.edu.cn.

Phone: +86-531-88363597. Fax: +86-531-88361008

thoroughly characterized by using various techniques including phase behavior observation, transmission electron microscopy (TEM), field emission scanning electron microscopy (FE-SEM), fluorescence spectra, fluorescence microscopy observations, Fourier transform infrared (FT-IR) spectroscopy, ^1H NMR, 2D ^1H - ^1H ROESY NMR, small-angle X-ray scattering (SAXS), X-ray diffraction (XRD) and rheological measurements. The hydrogels of α -CD/Tyloxapol are responsive to external stimuli including temperature, pH and guest molecules, and present gelation-induced quenching fluorescence emission property. The reason for this phenomenon may be that Tyloxapol molecules come into the cavity of α -CD and form the inclusion complexes. Due to the high electron density of the narrow cavity of α -CD, it induces the shift of the electron on the benzene ring which can weaken the π - π interaction and lead to the fluorescence quenching. Moreover, the hydrogel formed by α -CD/Tyloxapol is highly responsive to formaldehyde (HCHO). Addition of a small amount of HCHO can induce a gel-to-sol transition. Interestingly, once the gel transforms to solution, it becomes fluorescent. This makes α -CD/Tyloxapol hydrogel a promising candidate for HCHO detection and removal in home furnishings to reduce indoor environmental pollutants.

Introduction

Self-assembled supramolecular gels are a new class of important soft materials [1-4]. In the past decade, their fabrication has emerged as a hot research topic owing to their novel material properties and potential applications. Since supramolecular gels can respond to external stimuli such as temperature [5], light [6], protons [7] and metal ions [8], they are considered as “smart” materials and have found diverse applications in template synthesis, drug delivery [9], light harvesting [10], biomimetic systems [11] and electronics [12]. Usually, the supramolecular gels are constructed through supramolecular 3D networks formed by nanofiber assemblies which are made of amphiphilic molecules [13, 14] and research proves that the formation of hydrogels are attributed to the molecular self-assembly in solution by noncovalent interactions such as hydrogen bonding, π - π stacking, hydrophobic interactions, electrostatic interactions, and van der Waals interactions [15-18]. It is believed that study on the mechanism of hydrogel formation is very important for us to design the chemical structure of gelators and to adjust their performance.

Among different kinds of supramolecular gels, fluorescent ones, especially those constructed from π -conjugated gelators, have attracted considerable attention due to their promising applications in optoelectronics and fluorescence sensors [19]. Song et al. reported fluorescent hydrogels with ultrahigh water content (~99 wt %) and excellent mechanical strength by dissolving 4'-para-phenylcarboxyl-2, 2':6', 2''-terpyridine (PPCT) in KOH aqueous solution. The hydrogels present gelation-induced enhanced fluorescence emission and tunable nanostructure and viscoelasticity. In addition, they can adsorb formaldehyde, making them a promising candidate for HCHO removal in home furnishings [20]. Abbel et al. synthesized five fluorene-based co-oligomers and observed that subtle changes to the chemical structures can induce strong differences in their

aggregation behaviour. In concentrated solutions, two of the synthesized co-oligomers self-assemble into lyotropic organogels and the emission colour can be tuned by energy transfer to yield white emissive gels [21]. Therefore, it can be seen that the fluorescence properties of gel can be adjusted through the choice of different π -gelators.

Herein, we propose a new strategy for the design of multi-responsive fluorescent supramolecular gels based on inclusion complexation between α -cyclodextrin (α -CD) and Tyloxapol which is a nonionic surfactant containing benzene ring. For comparison, Trion X-100, which is a monomer of Tyloxapol, was also selected to form hydrogels under similar conditions. The properties of the hydrogels have been investigated in detail by visual inspection, fluorescence spectra, Fourier transform infrared (FT-IR) spectroscopy, X-ray diffraction (XRD), ^1H NMR, 2D ^1H - ^1H ROESY NMR, small-angle X-ray scattering (SAXS), rheological measurements and various imaging methods including transmission electron microscopy (TEM), field emission scanning electron microscopy (FE-SEM) and fluorescence microscopy. Moreover, the stimuli-responsiveness of α -CD/Tyloxapol hydrogels towards additives, pH, temperature, and solvent have also been demonstrated.

Experiment section

Materials

Tyloxapol and Trion X-100 (polyoxyethylene *tert*-octylphenyl ether, TX-100) were purchased from Sigma. Their chemical structures are shown in Figure 1. α -CD was purchased from Shandong Binzhou Zhiyuan Bio-Technology Co., Ltd. All the above reagents were used without further purification. Ultra-pure water used in the experiments was triply distilled by a quartz water purification system.

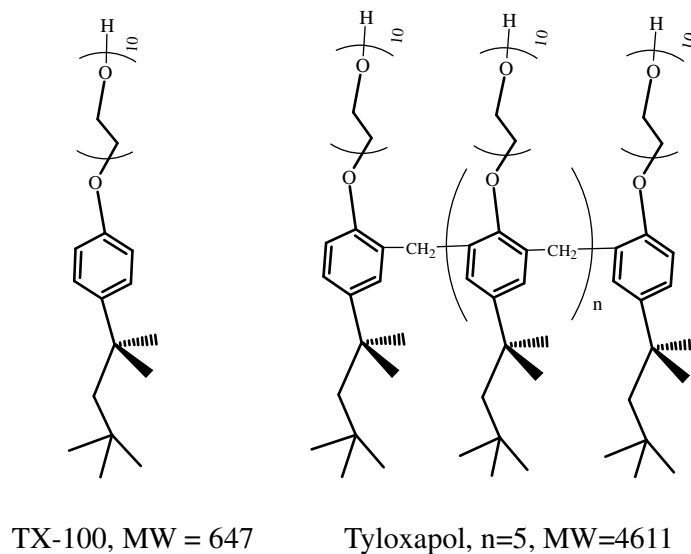


Figure 1 The chemical structures of TX-100 and Tyloxapol.

Methods and characterizations

For transmission electron microscopy (TEM) observations, about 5 μ L of hydrogel was placed on a TEM grid and the excess solution was wicked away with filter paper. The copper grid was freeze-dried and observed on a JEOL JEM-100 CXII (Japan) at an accelerating voltage of 80 kV. FE-SEM observations were carried out on a JEOL JSM-6700F. FT-IR spectrum was recorded on a VERTEX-70/70v spectrometer (Bruker Optics, Germany). XRD patterns of the freeze-dried samples were measured between 10 and 90° in the 2 θ scan mode (2.5° min⁻¹) using a Rigaku D/Max 2200-PC diffractometer with Cu K α radiation ($\lambda = 0.15418$ nm) and a graphite monochromator at room temperature. The fluorescence measurements were performed on a LS-55 spectrofluorometer (PerkinElmer, Waltham, MA, USA) with a quartz cell (1 \times 1 cm). OM) with a CCD camera (Panasonic Super Dynamic II WV-CP460). SAXS measurements were performed using an Anton-paar SAX Sess mc² system with Ni-filtered Cu K α radiation (1.54 Å) operating at 50 kV and 40 mA. ¹H NMR and 2D ¹H-¹H ROESY NMR spectra were measured using an API Bruker Avance

300 MHz NMR at ambient temperature.

Fluorescence Microscopy (FM) Observations.

A small amount of gel sample was homogeneously dispersed on a cover glass to generate a thin film, which was then freeze-dried in a vacuum extractor for several days. Observations were performed using an inverted microscope (model IX81, Olympus, Tokyo, Japan) equipped with a high-numerical-aperture 60 × oil-immersed objective lens (PlanApo, Olympus, Tokyo, Japan), a UV-mercury lamp (OSRAM, HBO, 103w/2, Germany), a mirror unit consisting of a 330–385 nm excitation filter, a 390–460 nm emission filter, and a 16 bit thermoelectrically cooled EMCCD (Cascade512B, Tucson, AZ, USA). The EMCCD was used for collecting the fluorescent images. Imaging acquisition and data analysis were performed using the MetaMorph software (Universal Imaging, Downingtown, PA, USA).

Rheological measurements.

The rheological measurements were carried out on an Anton Paar Physica MCR302 rheometer with cone-plate system (diameter, 25mm; cone angle 2°). Rheological property of hydrogels was measured. Before frequency sweep, an amplitude sweep at a fixed frequency of 1 Hz was operated to ensure the selected stress was in the linear viscoelastic region. The frequency sweep was carried out from 0.01-100 Hz at a fixed stress of 1 Pa. The samples were measured at 20.0±0.1 °C with the help of a cyclic water bath.

Results and discussion

Phase Behavior

To determine the formation condition of hydrogel, firstly, we studied the phase behavior of

α -CD/TX-100 and α -CD/Tyloxapol mixed systems. As shown in Fig 2A, when the concentration of α -CD is constant (100 mg mL^{-1}), the sample changes from solution to hydrogel and finally to two-phase with increasing concentration of TX-100. The formation of hydrogels was determined by “inverted-vial test” and photos of typical samples were given in Figure 2 B, C and D, respectively. It can be seen that only when the concentration of TX-100 is in the range of 5~15 mg mL^{-1} , α -CD/TX-100 mixed system can form hydrogels. This means that a suitable ratio of α -CD to TX-100 is needed for efficient inclusion between them and hence for the formation of the hydrogel.

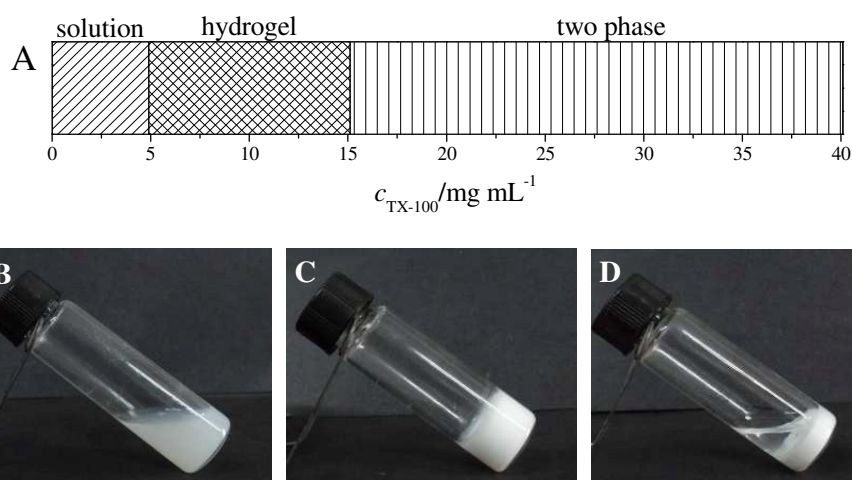


Figure 2 A) Phase behavior of α -CD/TX-100 mixed system after equilibrated at $20.0 \pm 0.1^\circ\text{C}$ for at least 4 weeks. The concentration of α -CD is fixed at 100 mg mL^{-1} while that of TX-100 is varied. B-D) Photographs of typical samples with 3 (B), 15 (C) and 40 (D) mg mL^{-1} TX-100, respectively.

Different with α -CD/TX-100 mixed system, in the case of α -CD/Tyloxapol with the same α -CD concentration (100 mg mL^{-1}), the two-phase region lies in between the solution phase and gel phase. The critical concentration of Tyloxapol for the formation of the hydrogels is 15 mg mL^{-1} , which is much higher than that of TX-100. Interestingly, the hydrogel region is quite wide, up to 40 mg mL^{-1} Tyloxapol (Figure 3 A). Photos of typical samples are given in Figure 3 B and C. Tyloxapol is oligomeric surfactant including seven TX-100 monomers which are connected by

methylene groups. The inclusion complexes formed by α -CD and PEO blocks of TX-100 and Tyloxapol result in the gelation of the solutions. Compared to TX-100, Tyloxapol has a larger hydrophobic part which can produce bigger steric effect. Thus the interaction between α -CD and Tyloxapol is suppressed, preventing the formation of supramolecular networks in lower Tyloxapol concentrations.

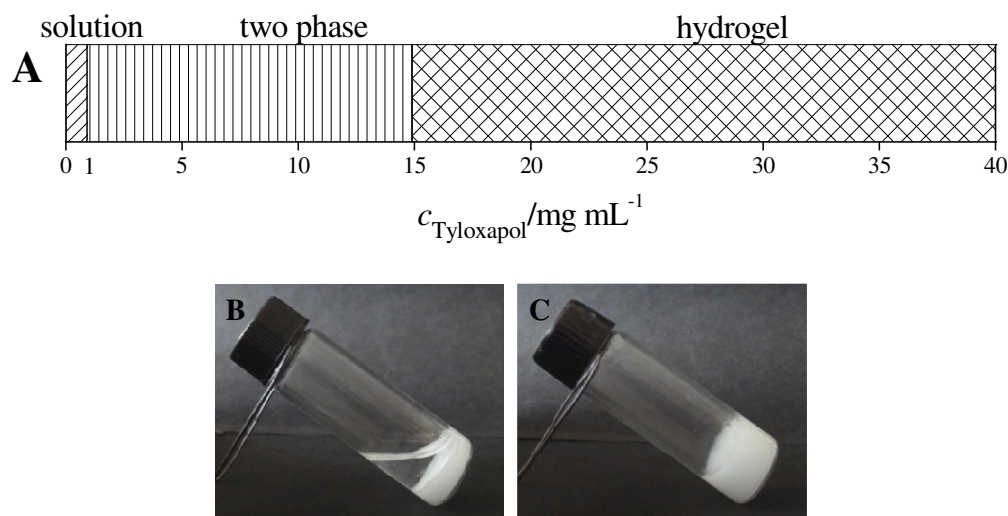
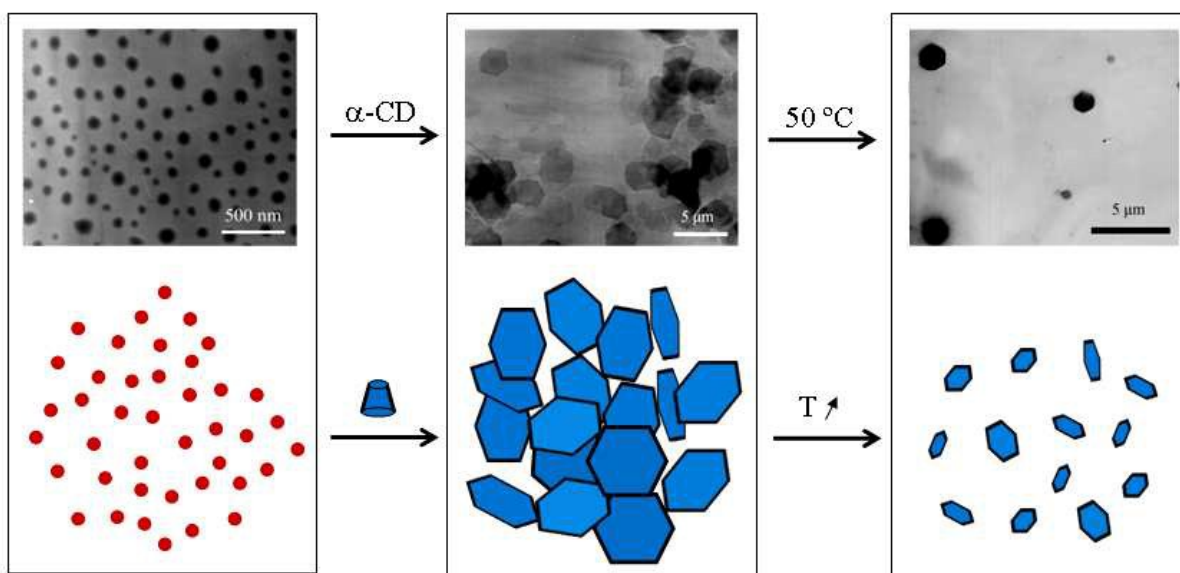


Figure 3. A) Phase behavior of α -CD/Tyloxapol mixed system after equilibrated at $20.0 \pm 0.1^\circ\text{C}$ for at least 4 weeks. The concentration of α -CD is fixed at 100 mg mL^{-1} while that of Tyloxapol is varied. B, C) Photographs of typical samples with 3 (B) and 15 (C) mg mL^{-1} Tyloxapol, respectively.

Microstructures

TEM and FE-SEM can be used to observe the morphology of various self-assembled structures in solutions and hydrogels to give their formation mechanism [22, 23]. Scheme 1 shows TEM results and the possible model for the inclusion interaction between α -CD and Tyloxapol and temperature-response of α -CD/Tyloxapol hydrogels. It can be seen that for the pure solution of 15 mg mL^{-1} Tyloxapol, they can form micelles [24, 25]. After addition of 100 mg mL^{-1} α -CD, polygons

appear which induce the formation of hydrogels. When the gel is heated, the number of the polygons becomes less and the size of the polygons becomes smaller and a gel-to-sol transition is noticed.



Scheme 1 TEM results and schematic showing of the possible model for the inclusion interaction between α -CD and Tyloxapol and temperature-response of α -CD/Tyloxapol hydrogels.

To further reveal the details of the microstructures in the gels, SEM observations were carried out and typical results are summarized in Figure 4. For all the samples from α -CD/TX-100 and α -CD/Tyloxapol mixed systems, closely-packed thick sheets have been detected. At a fixed concentration of α -CD (100 mg mL^{-1}) and the same concentration of TX-100 or Tyloxapol (15 mg mL^{-1}), the sheets in α -CD/TX-100 mixed system are larger and thicker compared to those in α -CD/Tyloxapol mixed system. It can be also seen that the sheets became smaller when the concentration of Tyloxapol is increased to 40 mg mL^{-1} (Figure 4 E F). This indicated that the concentration of TX-100 or Tyloxapol is an important factor to influence the formation of the hydrogels and the morphology of the microstructures.

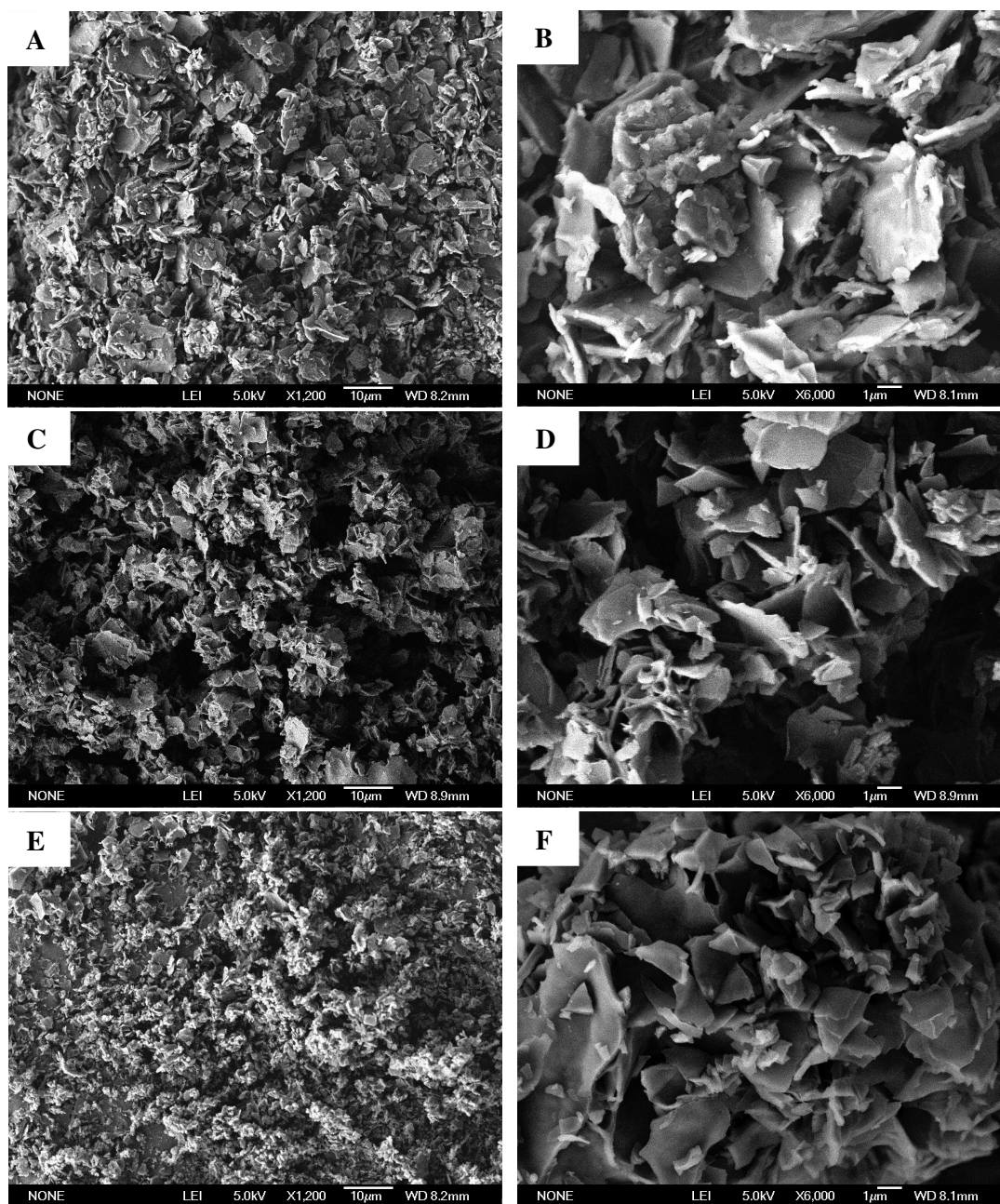


Figure 4 SEM images of the freeze-dried hydrogels from A, B) 100 mg mL^{-1} α -CD/ 15 mg mL^{-1} TX-100; C, D) 100 mg mL^{-1} α -CD/ 15 mg mL^{-1} Tyloxapol; and E, F) 100 mg mL^{-1} α -CD/ 40 mg mL^{-1} Tyloxapol, respectively.

Fluorescence property

The π - π interaction between the aromatic rings in the gels can be monitored by fluorescence spectra. Most planar π -conjugated gelators are highly emissive in solution state but become weak

emitters when self-assembled [26-28]. Thus, it is very useful for us to observe the fluorescence properties of our samples. First, the fluorescence spectra of Tyloxapol and TX-100 aqueous solutions were observed (Figure 5A). It can be seen that 15 mg mL^{-1} Tyloxapol aqueous solution is highly fluorescent under 350 nm excitation and the fluorescence intensity increased with increasing Tyloxapol concentration, (Figure S1). For 15 mg mL^{-1} TX-100 aqueous solution, however, no fluorescence has been detected. The fluorescence of Tyloxapol can be ascribed to the close packing of the seven benzene rings which produces a strong π - π interaction. While such effect is absent in TX-100. Then the fluorescence properties of two typical gel samples were analyzed. It can be seen that the sample of 100 mg mL^{-1} α -CD/ 15 mg mL^{-1} Tyloxapol is still fluorescent, as proved by the fluorescence spectrometer as well as hand-held UV lamp while the sample of 100 mg mL^{-1} α -CD/ 15 mg mL^{-1} TX-100 is still silent under both conditions (Figure 5B). Similar with the trend obtained from the dilute solutions, if the concentration of Tyloxapol is increased from 15 mg mL^{-1} to 40 mg mL^{-1} , the fluorescence intensity also increases (Figure S1). It should be noted that the fluorescence intensity of the gels is ~ 1 order of magnitude lower compared to that of aqueous solution. Similar phenomenon was also observed for 15 mg mL^{-1} Tyloxapol aqueous solution upon addition of α -CD where a gradual decrease of fluorescence intensity was noticed (Figure S2). This should originate from the complex formation between Tyloxapol and α -CD in the gel which prevents the close packing of the benzene groups. This assumption is further confirmed by the structural simulations by Material Studio software as shown in Figure 7, which reveals that after formation of inclusion complexes between α -CD and Tyloxapol, the steric hindrance increases and the chains of Tyloxapol become disordered.

The responses of the 100 mg mL^{-1} α -CD/ 15 mg mL^{-1} Tyloxapol hydrogel towards temperature

were also investigated. When heated above the gel-to-sol transition temperature (~ 40 °C), the opalescent hydrogel turns into a transparent solution and the fluorescence intensity increases significantly. Upon cooling, the fluorescence intensity declines continuously with time accompanied by a red shift (from 414 nm to 422 nm, Figure 6A). This phenomenon can be explained by the destruction of the α -CD/Tyloxapol inclusion complexes at high temperatures, which release free Tyloxapol with closely-packed benzene groups. Interestingly, the change of fluorescence intensity in the gel (20 °C) and sol (50 °C) state is reversible and can be repeated many times (Figure 6 B C), indicating that our gels have great potential to be used as thermal sensors and fluorescence molecular switch [20, 32].

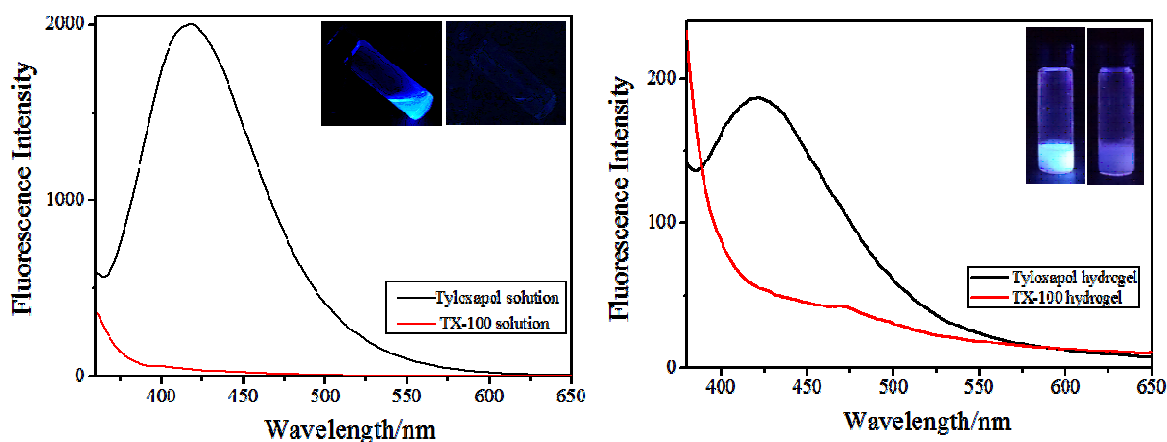


Figure 5 A) Fluorescence spectra of Tyloxapol and TX-100 aqueous solutions under 350 nm excitation. The concentration is 15 mg mL^{-1} in both cases. Insets are photos of the Tyloxapol (left) and TX-100 (right) aqueous solutions under 365 nm UV irradiation. B) Fluorescence spectra of 100 mg mL^{-1} α -CD/ 15 mg mL^{-1} Tyloxapol and 100 mg mL^{-1} α -CD/ 15 mg mL^{-1} TX-100 hydrogels. Insets are photos of Tyloxapol-based (left) and TX-100-based (right) gels under 365 nm UV irradiation.

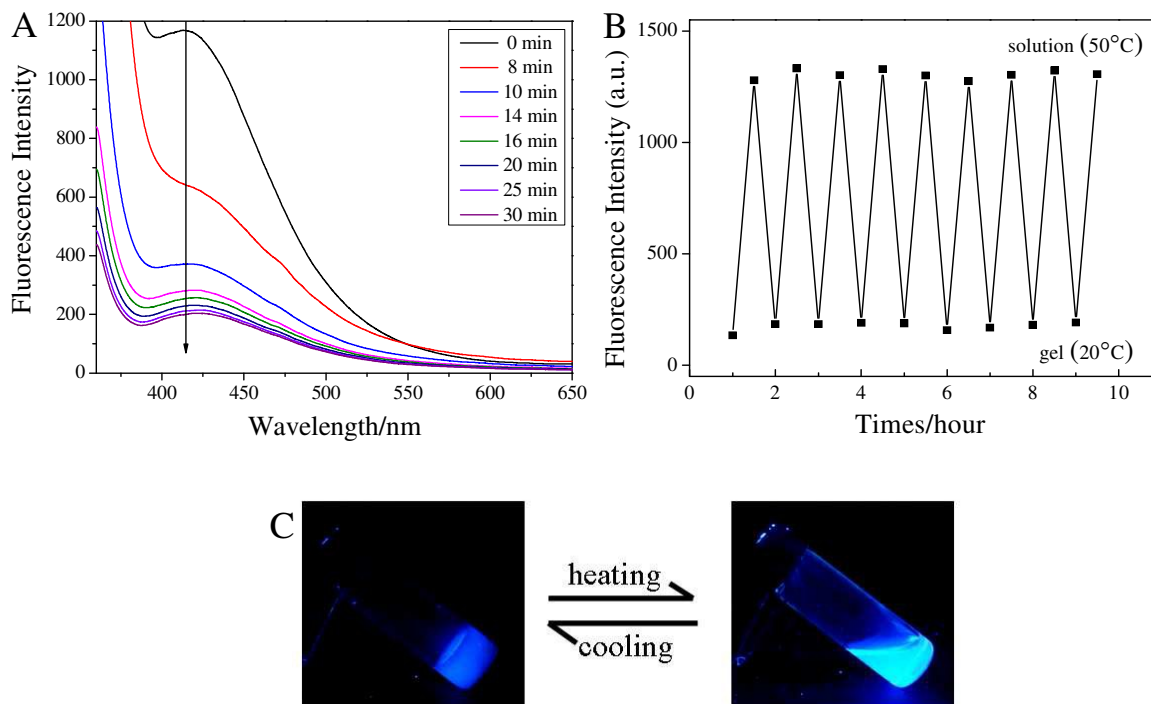


Figure 6 A) Change of the fluorescence spectra of the hot solution (50 °C) of 100 mg mL⁻¹ α -CD/15 mg mL⁻¹ Tyloxapol hydrogel upon cooling. $\lambda_{\text{ex}} = 350$ nm. B, C) Variation of the emission intensity at 414 nm (B) and photographs under 365 nm UV irradiation (C) of the hydrogel during sol-gel transition (50 °C to 20 °C).

Due to the fluorescent characteristics, the microstructures of the α -CD/Tyloxapol gels can be also monitored by conventional fluorescence microscope. Typical images of two gel samples with compositions of 100 mg mL⁻¹ α -CD/15 mg mL⁻¹ Tyloxapol and 100 mg mL⁻¹ α -CD/40 mg mL⁻¹ Tyloxapol without and with a 435 nm-485 nm filter are shown in Figure 8. Without filter (i.e., under white light), the gels appear as discrete islands separated by darker regions (Figure 8, A C). When a 435 nm-485 nm filter was applied, however, the islands become silent and the surroundings become bright (Figure 8 B D). According to the observations from fluorescence spectra mentioned above, we concluded that the islands are mainly composed of α -CD/Tyloxapol inclusion complexes while the surroundings mainly consist of surfactant unimers which have a much higher fluorescence

intensity. Similar phenomenon was also detected by confocal fluorescence microscopy observations on the gel of 100 mg mL^{-1} α -CD/ 15 mg mL^{-1} Tyloxapol (Figure 9).

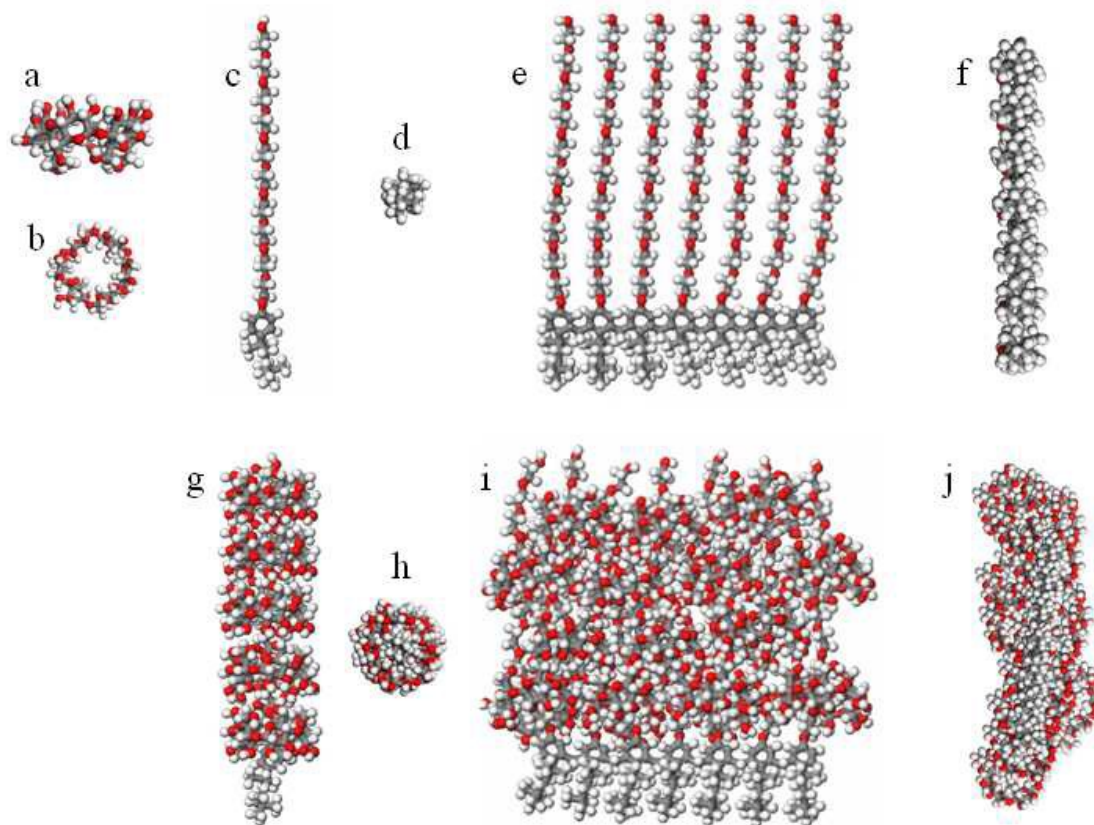


Figure 7 The ball-and-stick models obtained by Material Studio software of α -CD (a, b), Trion X-100 (c, d) and Tyloxapol (e, f) molecules and the inclusions formed by α -CD with Trion X-100 (g, h) or Tyloxapol (i, j), respectively. Red globes represent oxygen atoms; gray globes, carbon atoms; white globes, hydrogen atoms. a, c, e, g, i: side view; b, d, f, h, j: top view.

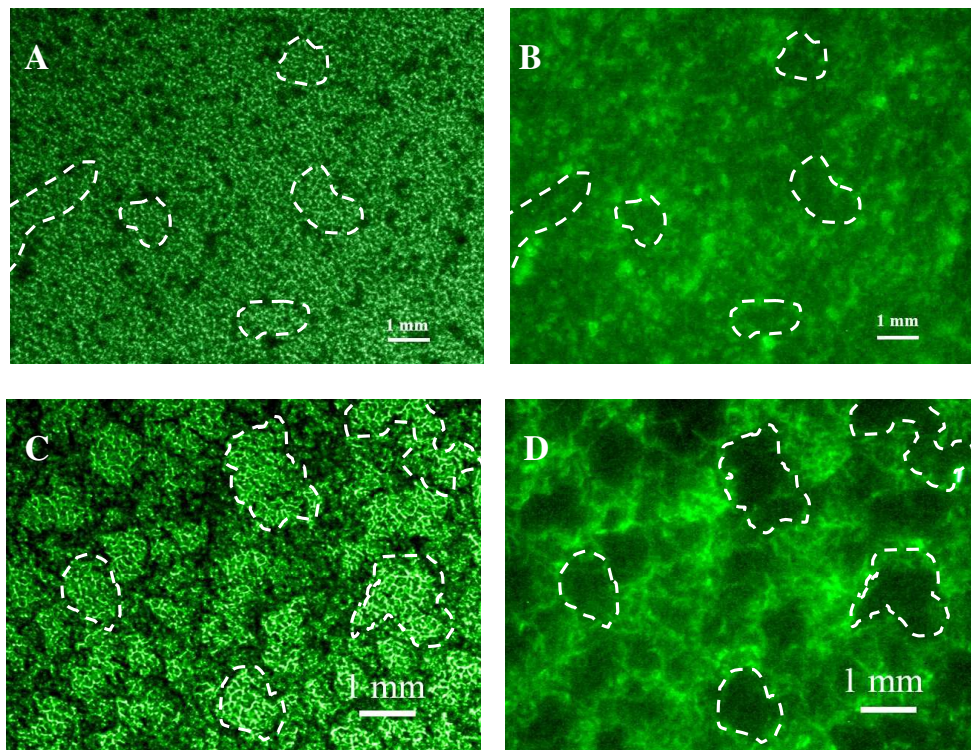


Figure 8 Fluorescence microscopy images of supramolecular hydrogel formed by 100 mg mL^{-1} α -CD/ 15 mg mL^{-1} Tyloxapol (A, B) and 100 mg mL^{-1} α -CD/ 40 mg mL^{-1} Tyloxapol (C, D) without (A, C) and with a 435 nm-485 nm filter (B, D), respectively. The green colours were set up artificially for easier viewing and the original black-and-white images are shown in Figure S3.

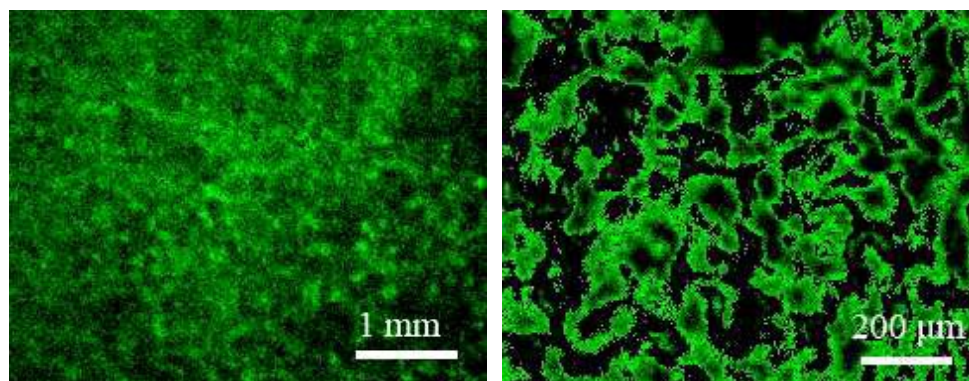


Figure 9 Confocal fluorescence microscopy images of supramolecular hydrogel formed by 100 mg mL^{-1} α -CD/ 15 mg mL^{-1} Tyloxapol at different magnifications.

XRD analysis and $^1\text{H-NMR}$, FT-IR spectra

In order to get information about the degree of crystallinity of the inclusion complexes, XRD measurements of α -CD/Tyloxapol and α -CD/TX-100 xerogels were performed and the results are shown in Figure 10. It can be seen that α -CD gives a variety of diffraction peaks corresponding to a cage type structure [33]. For Tyloxapol and TX-100, only a broad peak was detected which means the chains are in disordered states. Once the inclusion complexes form between Tyloxapol or TX-100 and α -CD, a sharp reflection emerged at $2\theta = 19.8$ which represents the channel type structure of crystalline necklace-like complex of α -CD and Tyloxapol or TX-100 [33]. Thus, it can be concluded that the inclusion complexes formed by α -CD and PEO blocks of TX-100 and Tyloxapol are thought to aggregate into microcrystals [34], which act as physical crosslinks and induce formation of a supramolecular network, consequently resulting in the gelation of the solutions.

Moreover, it is well-known that α -CD can form inclusion complexes with PEO blocks [33]. In order to demonstrate whether α -CD can form inclusion complexes with PEO blocks of Tyloxapol, we used 2D ^1H - ^1H ROESY to confirm the formation of inclusion complexes between α -CD and Tyloxapol, signal of H3, H5 inside the cavity of α -CD shows no correlation peaks with alkyl chain of Tyloxapol, and shows correlation peaks with $-(\text{CH}_2-\text{CH}_2-\text{O})-$ group of Tyloxapol (Figure S4). Thus, it can be speculated that α -CD can only form inclusion complexes with the $-(\text{CH}_2-\text{CH}_2-\text{O})-$ group of Tyloxapol and the end of tertiary butyl of alkyl chain is too big to form inclusion complexes with α -CD. Furthermore, small-angle X-ray scattering (SAXS) measurement has been done (Figure S5), the results showed the long range order of the complexes in the hydrogels and the scattering peaks at 1.85, 2.85 and 5.21 nm^{-1} are corresponding to the d spacing of 3.4, 2.2 and 1.2

nm, respectively. The value of 3.4 nm is a little less than the chain strength of Tyloxapol (4.3 nm), this may be because that polyoxyethylene is flexible, it maybe crooked in the network of hydrogel (Figure 7i) or it maybe represent the widths of seven benzenes for one Tyloxapol molecule (3.3 nm). The *d* spacing of 2.2 nm may be the stacking of α -CD and 1.2 nm can be ascribed to the length of the hydrophobic parts of alkyl chain of two Tyloxapols.

Then, we use two ways to calculate how many cyclodextrins are being threaded per side-chain of Tyloxapol. Firstly, we separated the precipitation and solution of the sample of 100 mg mL⁻¹ α -CD/5 mg mL⁻¹ Tyloxapol, then dissolved the freeze-dried precipitation into DMSO-d₆. As is shown in Figure 11, by calculating the proportion of the integrations of α -CD (H1 protons) and the integrations of Tyloxapol (CH₃ protons), it can be confirmed that the host-guest stoichiometries is 2:1 (1/6: 0.82/9). Secondly, we verified the host-guest stoichiometries in another way by comparing the chemical shifts change of α -CD H5 as a function of the concentration of Tyloxapol from ¹HNMR results (Figure S6), it can be seen that the largest shift occurs when $m_{\alpha\text{-CD}} : m_{\text{Tyloxapol}} = 10 : 3.5$ ((10/973) : (3.5/4611) = 13.5,) 13.5/7 (seven polyoxyethylene ether chains per Tyloxapol) ≈ 2 . It can be seen that the results obtained by these two methods are consistent, which means that each polyoxyethylene ether chain of Tyloxapol needs two α -CD and one Tyloxapol molecule can interact with fourteen α -CD molecules to form inclusion complex.

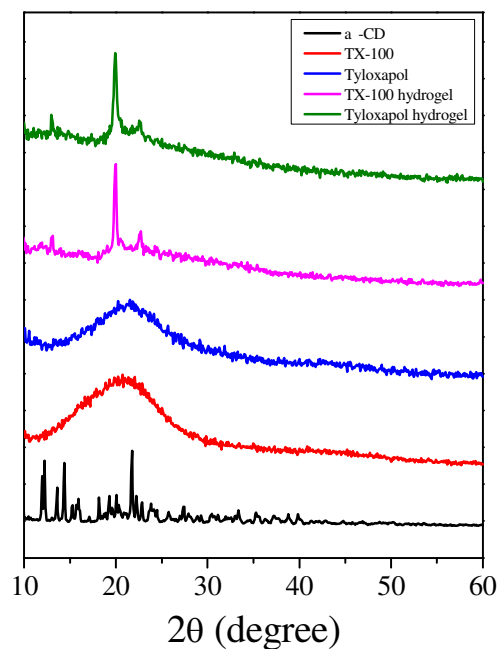


Figure 10 XRD patterns of the xerogel of (a) α -CD, (b) TX-100, (c) Tyloxapol, (d) 100 mg mL^{-1} α -CD/ 15 mg mL^{-1} TX-100, (e) 100 mg mL^{-1} α -CD/ 15 mg mL^{-1} Tyloxapol.

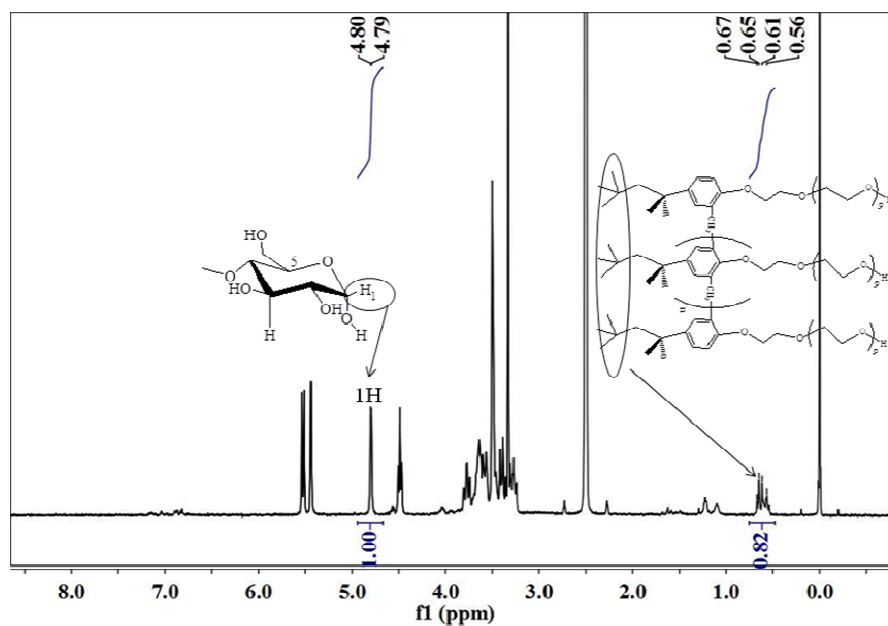


Figure 11. ^1H NMR spectra of 100 mg mL^{-1} α -CD/ 5 mg mL^{-1} Tyloxapol precipitates in DMSO- d_6 .

FT-IR spectroscopy is a powerful method for characterizing the interactions within supramolecular assemblies [18]. The stretching vibration at 1643 cm^{-1} is related to carbonyl groups

and the peak at 1030 cm^{-1} is in agreement with the stretching vibration of C-O bond of α -CD (Figure 12 a). It can be also seen that the asymmetric and symmetric methylene stretching bands are located at 2951 and 2869 cm^{-1} for TX-100 and Tyloxapol (Figure 12 b, c), respectively. The wide peak between 3350 – 3500 cm^{-1} is well-known for symmetric and antisymmetric O-H stretching modes. It should be noted that the peak of O-H shifts from 3478 cm^{-1} to a lower frequency at 3384 cm^{-1} or 3335 cm^{-1} when α -CD was added into Tyloxapol or TX-100 solutions to form hydrogels (Figure 12 d, e). It can be conclude that the threading of α -CD onto Tyloxapol or TX-100 not only prompted by inclusion interaction between α -CD and PEO, but also hydrogen bonding between adjacent α -CD and between α -CD and PEO.

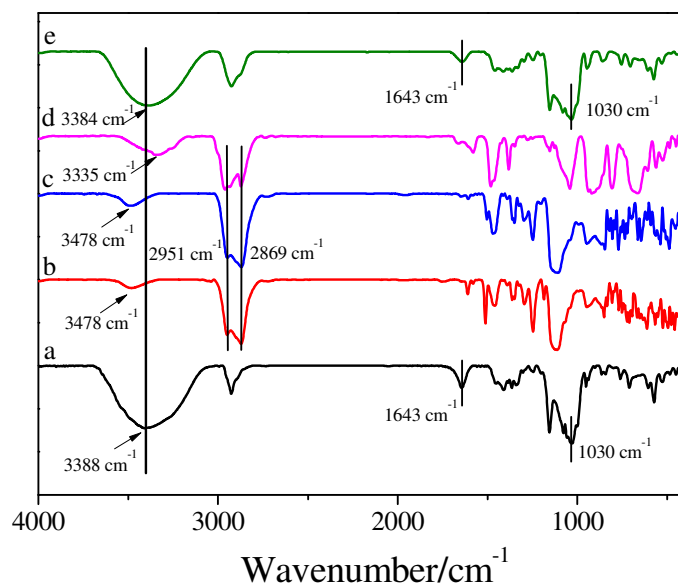


Figure 12 FT-IR patterns of the xerogel of (a) α -CD, (b) TX-100, (c) Tyloxapol, (d) 100 mg mL^{-1} α -CD/ 15 mg mL^{-1} TX-100, (e) 100 mg mL^{-1} α -CD/ 15 mg mL^{-1} Tyloxapol.

Rheological properties

Rheological behavior is one of the most important methods to characterize viscoelasticity of hydrogel [34]. The plateau where complex modulus is independent of the shear stress is considered

to be the linear viscoelastic region. Generally, samples are always ensured that they are within the linear viscoelastic region before carrying out the frequency oscillatory measurement [35]. As is shown in Figure 13 A and C, it can be seen that both α -CD/TX100 and α -CD/Tyloxapol hydrogels show the linear viscoelastic region. Moreover, the storage modulus (G') is much greater than loss modulus (G'') which exhibits an elastic dominant property, demonstrating a solid-like rheological property. For α -CD/TX-100 hydrogels, G' first increases and then decreases with increasing TX-100 concentration, which is consistent with the phase sequence where the hydrogel first forms but then phase separated with continuous addition of TX-100 (Figure 2 A). For α -CD/Tyloxapol hydrogels, however, G' keeps increasing when the concentration of Tyloxapol is increased from 15 mg mL⁻¹ to 40 mg mL⁻¹, which is also consistent with the phase sequence (Figure 3 A). At the same surfactant concentration (for example, 15 mg mL⁻¹), the strength of TX-100 gel is stronger than the Tyloxapol gel (Figure S7). This can be ascribed to the relatively smaller steric hindrance for TX-100 for α -CD inclusion compared to Tyloxapol, which causes a stronger interaction between TX-100 with α -CD and leads to the formation of more uniform microstructures as proved by fluorescence microscopy observations (Figure 8). Scheme 2 gives the possible models for the self-assembly of α -CD/TX-100 and α -CD/Tyloxapol.

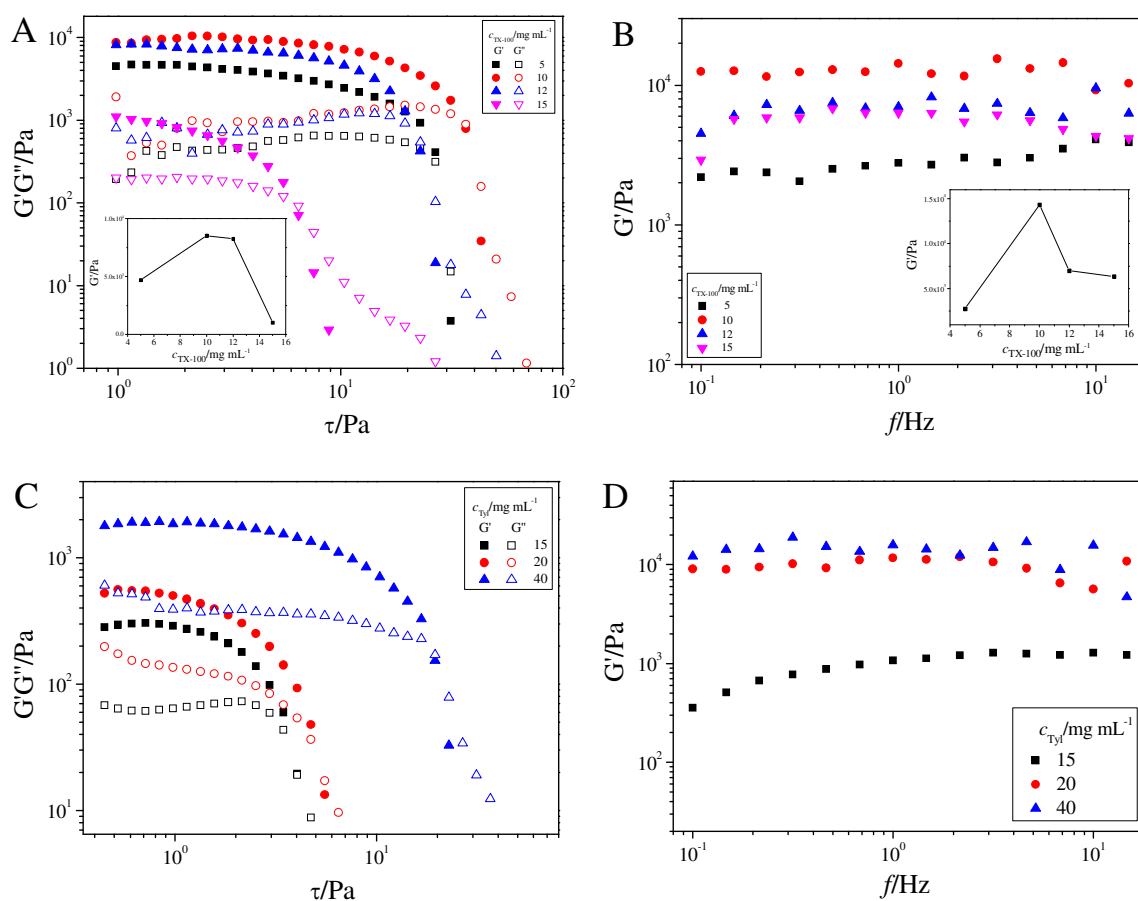
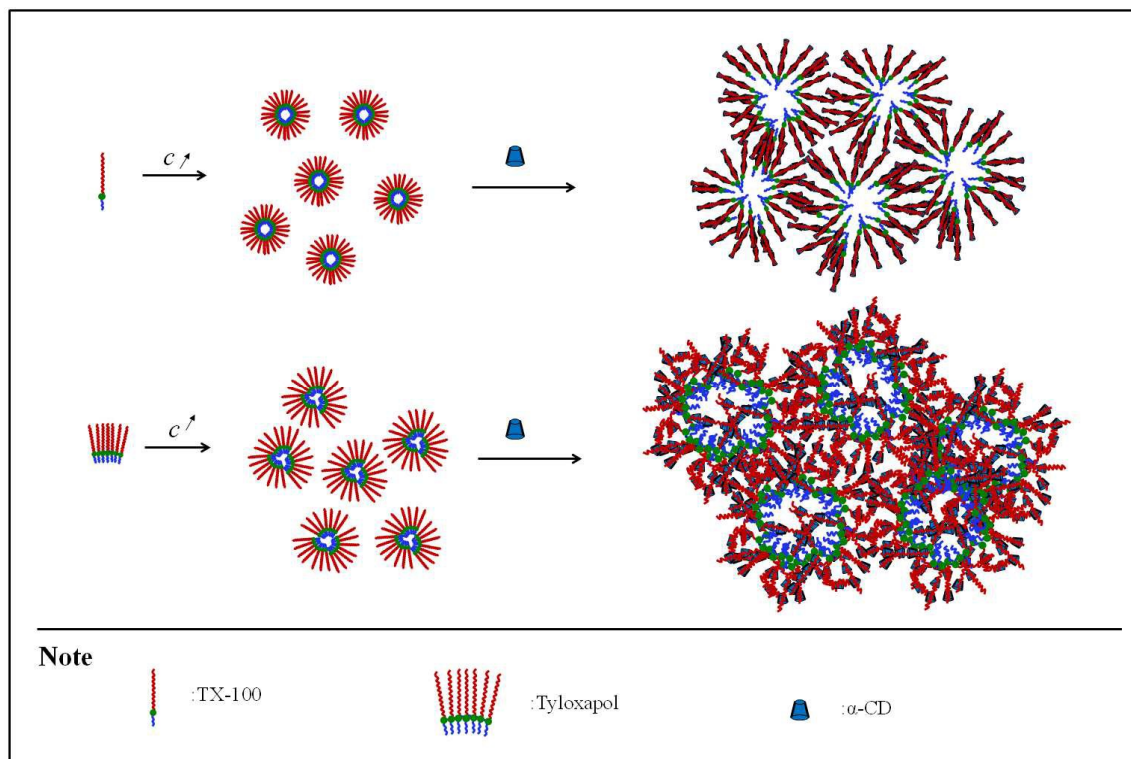


Figure 13 Rheological results of hydrogels with different concentration of TX-100 (A, B) or Tyloxapol (C, D) and fixed concentration of α -CD at 100 mg mL⁻¹: (A, C) G' and G'' as a function of the applied stress at a constant frequency (1.0 Hz) and (B, D) variation of G' as a function of frequency. Insets in A, B are the variation of G' as a function of the concentration of TX-100 in stress sweeping ($f = 1$ Hz) and frequency sweeping ($\tau = 1$ Pa).



Scheme 2 Schematic diagram of the possible model of TX100 and Tyloxapol aggregates and the networks of hydrogels of α -CD/TX100 and α -CD/Tyloxapol.

Multiple responses of the α -CD/Tyloxapol hydrogel

It is well established that the physical and chemical properties of CDs are responsive to multiple external stimuli such as temperature, pH, and guest molecules [36]. In most cases, the host-guest complexes based on CDs either self-assemble via hydrophobic interactions [37, 38] or lose the self-assembling abilities due to the increased solubility in water [39, 40]. Thus, it can be expected that our α -CD/Tyloxapol hydrogels are multi-responsive. Besides the temperature responsiveness as mentioned above, response of α -CD/Tyloxapol hydrogels towards pH and small molecule additives were tested and the results are summarized in Figure 14 and Figure S8. It can be seen that when NaOH was added, the opalescent hydrogel becomes clear at pH 14, which is close to the pKa of α -CD (12.2). The ionization of α -CD at high pH would significantly destabilize the α -CD/Tyloxapol

complex and the polygon-shaped structure due to electrostatic repulsion as well as the disappearance of H-bonds among CD molecules. Adding HCl (up to pH = 2) induced a transition from the opalescent hydrogel to opalescent sol accompanied by a slight increase of the fluorescence intensity. Furthermore, it is interesting to find that our hydrogel can also respond to toxic substance such as formaldehyde (HCHO) and toluene, that is because HCHO is small molecule which is a strongly competitive guest for α -CD and has a strong binding constant with α -CD, thus, HCHO can snatch the host molecule (α -CD) replace Tyloxapol into the cavity of α -CD easily to form α -CD/HCHO inclusion complex, affect the inclusion behavior of α -CD and Tyloxapol and eventually destroyed the structure of α -CD/Tyloxapol hydrogels. [41,42]. This makes hydrogel a promising candidate for HCHO detection and removal in home furnishings to reduce indoor environmental pollutants and/or for toluene removal in swage treatment [20, 43, 44]. It is anticipated this new type of α -CD/Tyloxapol hydrogels are also responsive to other kinds of α -CD guests.

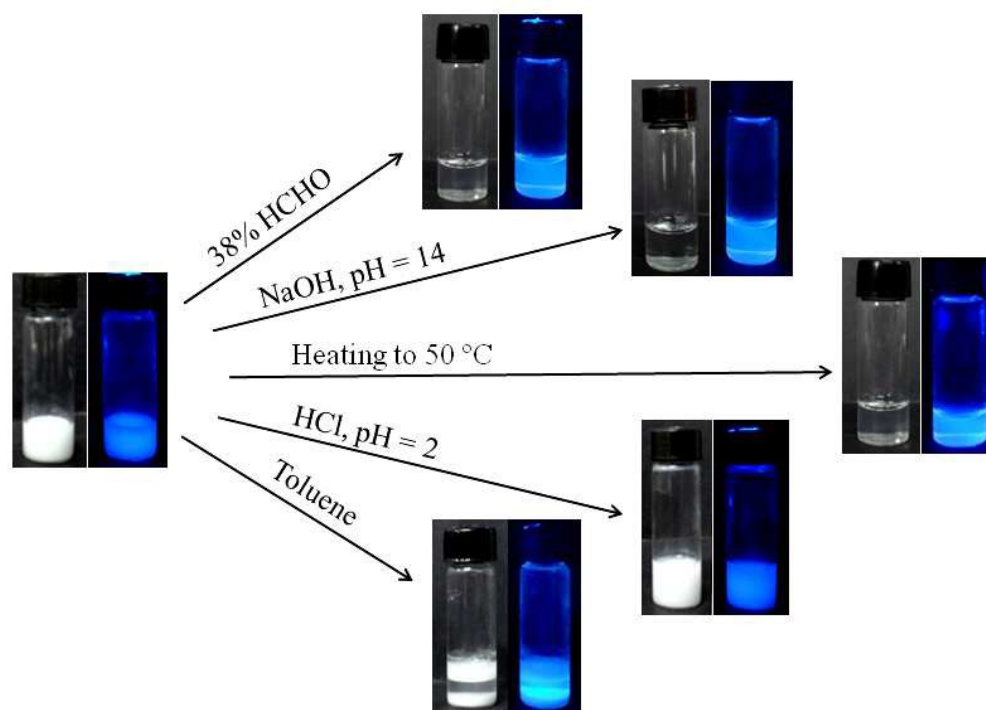


Figure 13 Response of 100 mg mL^{-1} α -CD/ 15 mg mL^{-1} Tyloxapol hydrogel towards additives, pH,

temperature and solvent.

Conclusions

Based on host-guest interaction between α -CD and Tyloxapol, fluorescent supramolecular hydrogels were constructed and fully characterized by phase behavior study, fluorescence spectra, TEM, FE-SEM, FT-IR, XRD, ^1H NMR, SAXS and rheological measurements. The results revealed that our α -CD/Tyloxapol hydrogels have good fluorescent properties and more importantly, the fluorescent properties can be adjusted by changing the mixing molar ratio of α -CD to Tyloxapol. Moreover, the α -CD/Tyloxapol hydrogels are responsive to external stimuli such as small molecule additives, pH and temperature, which can significantly broaden their potential applications. Specifically, the responsiveness of our α -CD/Tyloxapol hydrogels towards HCHO can be used for the detection and removal of HCHO in home furnishings, which is beneficial to human health.

Acknowledgement

We gratefully acknowledge the financial support from the National Natural Science Foundation of China (21203109) and Ji'nan Youth Science and Technology Star Program (2013040). TK and RH were supported from the sources of the National Science Centre according to the decision number DEC-2013/08/W/NZ1/00687 (SYMFONIA grant).

References

- [1] Z. Zhao, J. Lam, and B. Tang, *Soft Matter*, 2013, **9**, 4564-4579.
- [2] J. Puigmartí-Luis, V. Laukhin, A Pérez del Pino, J. Vidal-Gancedo, C. Rovira, E. Laukhina, D. Amabilino, *Angew. Chem. Int. Ed.*, 2007, **46**, 238-241.

- [3] Z. Yang, P. L. Ho, G. Liang, K. H. Chow, Q. Wang, Y. Cao, B. Xu, *J. Am. Chem. Soc.*, 2007, **129**, 266-267.
- [4] S. Song, R. Dong, D. Wang, A. Song, J. Hao, *Soft Matter*, 2013, **9**, 4209-4218.
- [5] S. Das, S. Varghese and N. S. S. Kumar, *Langmuir*, 2010, **26**, 1598-1609.
- [6] C. Wang, Q. Chen, F. Sun, D. Zhang, G. Zhang, Y. Huang, R. Zhao and D. Zhu, *J. Am. Chem. Soc.*, 2010, **132**, 3092-3096.
- [7] X. Chen, Z. Huang, S.-Y. Chen, K. Li, X.-Q. Yu and L. Pu, *J. Am. Chem. Soc.*, 2010, **132**, 7297-7299.
- [8] M.-O. M. Piepenbrock, G. O. Lloyd, N. Clarke and J. W. Steed, *Chem. Rev.*, 2010, **110**, 1960-2004.
- [9] H. Tang, X. Duan, X. Feng, L. Liu, S. Wang, Y. Li and D. Zhu, *Chem. Commun.*, 2009, **6**, 641-643.
- [10] C. Vijayakumar, V. K. Praveen and A. Ajayaghosh, *Adv. Mater.*, 2009, **21**, 2059-2063.
- [11] A. Shome, S. Dutta, S. Maiti and P. K. Das, *Soft Matter*, 2011, **7**, 3011-3022.
- [12] S. S. Babu, S. Prasanthkumar and A. Ajayaghosh, *Angew. Chem. Int. Ed.*, 2012, **51**, 1766-1776.
- [13] K. Liu, N. Yan, J. Peng, J. Liu, Q. Zhang, Y. Fang, *J. Colloid Interface Sci.*, 2008, **327**, 233-242.
- [14] M. Mukai, H. Minamikawa, M. Aoyagi, *J. Colloid. Interf. Sci.*, 2013, **395**, 154-160.
- [15] K. Trickett, J. Eastoe, *Adv. Colloid. Interf. Sci.*, 2008, **144**, 66-74.
- [16] Y. Zhang, X. Xin, J. Shen, W. Tang, Y. Ren, L. Wang, *RSC Advances*, 2014, **4**, 62262-62271.
- [17] X. Sun, X. Xin, N. Tang, L. Guo, L. Wang, and G. Xu, *J. Phys. Chem. B*, 2014, **118**, 824-832.
- [18] Y. Wang, X. Xin, W. Li, C. Jia, L. Wang, J. Shen, G. Xu, *J. Colloid. Interf. Sci.*, 2014,

431,82-89.

[19] Y. Gong, Q. Hu, N. Cheng, T. Wang, W. Xu, Y. Bi and L. Yu, *J. Mater. Chem. C*, 2015, **3**, 3273-3279.

[20] S. Song, A. Song, L. Feng, G. Wei, S. Dong, and J. Hao, *ACS Appl. Mater. Interfaces*, 2014, **6**, 18319-18328.

[21] R. Abbel, R. van der Weegen, W. Pisula, M. Surin, P. Leclère, R. Lazzaroni, and A. P. Schenning, *Chem. Eur. J.*, 2009, **15**, 9737-9746.

[22] R. Xue, X. Xin, L. Wang, J. Shen, F. Ji, W. Li, C. Jia, G. Xu, *Phys. Chem. Chem. Phys.*, 2015, **17**, 5431-5440.

[23] J. Shen, X. Xin, Y. Zhang, L. Song, L. Wang, W. Tang, Y. Ren, *Carbohydr. Polym.*, 2015, **117**,592-599.

[24] X. Xin, Y. Zhu, X. Cao, G. Xu, *J. Surfact. Deterg.*, 2014, **17**,71-83.

[25] Y. Zhu, G. Xu, X. Xin, H. Zhang, X. Shi. *J. Chem. Eng. Data*, 2009, **54**, 989-995.

[26] S. S. Babu, V. K. Praveen, A. Ajayaghosh. *Chem. Rev.*, 2014, **114**, 1973-2129.

[27] A. Ajayaghosh, V. K. Praveen, *Acc. Chem. Res.*, 2007, **40**, 644-656.

[28] S. S. Babu, S. Prasanthkumar, A. Ajayaghosh, *Angew. Chem. Int. Ed.*, 2012, **51**, 1766- 1776.

[29] W. Rettig, B. Zietz, *Chem. Phys. Lett.*, 2000, **317**, 187-196

[30] C. Zhan, D. Wang, *J. Photoch. Photobio. A*, 2002, **147**, 93-101.

[31] S. Ionescu, M. Hillebrand, *Chem. Phys.*, 2003, **293**, 53-64.

[32] C. Wang, D. Zhang, J. Xiang, D. Zhu, *Langmuir*, 2007, **23**, 9195 -9200.

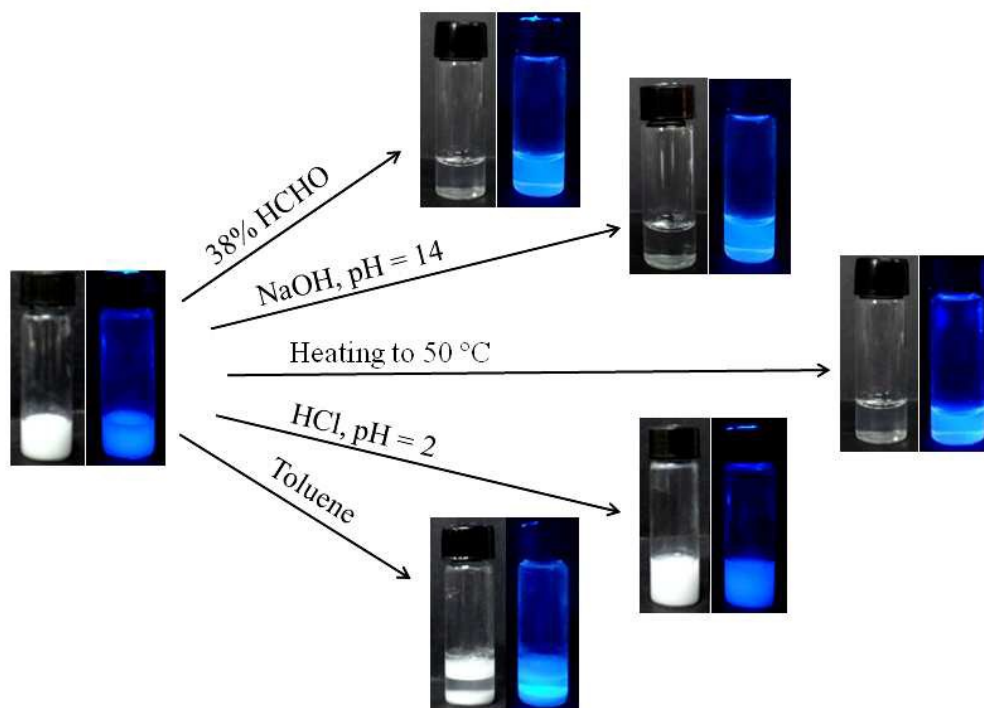
[33] Z. Feng, S. Zhao, *Polymer*, 2003, **44**, 5177-5186.

- [34] J. Shen, G. Xu, X. Xin, L. Wang, Z. Song, H. Zhang, L. Tong, Z. Yang, *RSC Advances*, 2015, DOI: 10.1039/c5ra04351d.
- [35] L. Xu, G. Xu, T. Liu, Y. Chen, H. Gong, *Carbohydr. Polym.*, 2013, **92**, 516-522.
- [36] L. Jiang, Y. Yan and J. Huang, *Soft Matter*, 2011, **7**, 10417- 10423.
- [37] C. Zhou, X. Cheng, Q. Zhao, Y. Yan, J. Wang, J. Huang, *Scientific reports*, 2014, **4**, 7533.
- [38] L. Jiang, Y. Yan, J. Huang, *Adv. Colloid. Interf. Sci.*, 2011, **169**, 13-25.
- [39] Y. Yan, L. Jiang and J. Huang, *Phys. Chem. Chem. Phys.*, 2011, **13**, 9074-9082.
- [40] L. Jiang, Y. Yan, M. Drechsler, and J. Huang, *Chem. Commun.*, 2012, **48**, 7347-7349.
- [41] J. Hu, X. Wu, W. Zeng, *J Controlled Release*, 2011, **152**, 211-213.
- [42] S. Li, L. Zhang, B. Wang, *Soft matter*, 2015, **11**, 1767-1777.
- [43] T. Salthammer, S. Mentese, R. Marutzky, *Chem. Rev.*, 2010, **110**, 2536-2572.
- [44] J. Yu, X. Li, Z. Xu, W. Xiao, *Environ. Sci. Technol.*, 2013, **47**, 9928-9933.

Manipulation of Multiple-responsive Fluorescent Supramolecular Materials Based on Inclusion Complexation of Cyclodextrins With Tyloxapol

Jinglin Shen, Jinyu Pang, Tomasz Kalwarczyk, Robert Hołyst, Xia Xin^{*}, Guiying Xu, Xiaoyu Luan,

Yingjie Yang



Response of 100 mg mL^{-1} α -CD/ 15 mg mL^{-1} Tyloxapol hydrogel towards additives, pH, temperature and solvent.

^{*} Author to whom correspondence should be addressed, E-mail: xinx@sdu.edu.cn.

Phone: +86-531-88363597. Fax: +86-531-88361008